Article

Multiyear Measurements on $\Delta^{17}O$ of Stream Nitrate Indicate High Nitrate Production in a Temperate Forest

Shaonan Huang, Fan Wang, Emily M. Elliott, Feifei Zhu, Weixing Zhu, Keisuke Koba, Zhongjie Yu, Erik A. Hobbie, Greg Michalski, Ronghua Kang, Anzhi Wang, Jiaojun Zhu, Shenglei Fu, and Yunting Fang*

Cite This: *Environ. Sci. Technol.* 2020, 54, 4231−4239

Read Online

ACCESS | 📊 Metrics & More | 📰 Article Recommendations | SI Supporting Information

ABSTRACT: Nitrification is a crucial step in ecosystem nitrogen (N) cycling, but scaling up from plot-based measurements of gross nitrification to catchments is difficult. Here, we employed a newly developed method in which the oxygen isotope anomaly ($\Delta^{17}O$) of nitrate (NO_3^-) is used as a natural tracer to quantify in situ catchment-scale gross nitrification rate (GNR) for a temperate forest from 2014 to 2017 in northeastern China. The annual GNR ranged from 71 to 120 kg N ha^{-1} yr^{-1} (average 94 ± 10 kg N ha^{-1} yr^{-1}) over the 4 years in this forest. This result and high stream NO_3^- loss (4.2−8.9 kg N ha^{-1} yr^{-1}) suggest that the forested catchment may have been N-saturated. At the catchment scale, the total N output of 10.7 kg N ha^{-1} yr^{-1}, via leaching and gaseous losses, accounts for 56% of the N input from bulk precipitation (19.2 kg N ha^{-1} yr^{-1}). This result indicates that the forested catchment is still retaining a large fraction of N from atmospheric deposition. Our study suggests that estimating in situ catchment-scale GNR over several years when combined with other conventional flux estimates can facilitate the understanding of N biogeochemical cycling and changes in the ecosystem N status.
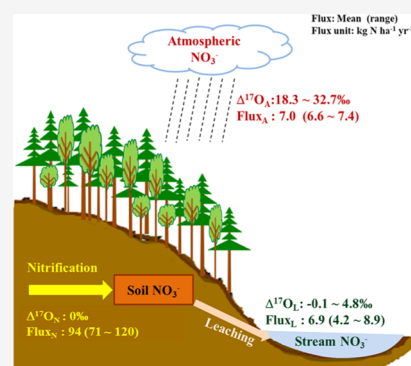
1. INTRODUCTION

Human activities have greatly altered the global nitrogen (N) cycle and dramatically increased the atmospheric N deposition.[1,2] Although N deposition can increase the primary productivity of N-limited ecosystems, excess N loads can adversely affect the terrestrial ecosystems through acidification of soils and streams, eutrophication of water bodies, and increased greenhouse gas emissions.[3−7] Nitrification, a microbial process of oxidizing ammonium (NH_4^+) to nitrate (NO_3^-), is a crucial step in the N cycling controlling these detrimental impacts induced by N deposition.[3] Nitrate is highly mobile and can readily leach into streams, causing base cation depletion, soil acidification, and aquatic eutrophication.[3,4] In addition, nitrate is the substrate for denitrification, a major biological process causing emissions of the greenhouse gas nitrous oxide (N_2O), which is also produced during nitrification. However, nitrification rates at an ecosystem scale remain poorly constrained. The gross nitrification rate (GNR) is the total NO_3^- production rate, which can better reflect the internal N cycling than net nitrification, especially in forest ecosystems where net nitrification rates are very low but NO_3^- production and consumption are significant.[8,9]

Methodological difficulties (e.g., scaling up from plot-based measurements to the ecosystem level) have limited estimates of the GNR at an ecosystem scale. Gross nitrification rates have traditionally been estimated with the ^{15}N pool dilution technique or with the barometric process separation (BaPS)

technique.[8,10] However, the ^{15}N pool dilution method introduces labeled ^{15}N to the soil (often undesirable in research settings), while the BaPS method requires several assumptions and is only applicable to well-aerated soils. In addition, both the ^{15}N pool dilution and the BaPS method should only be extrapolated cautiously beyond individual soil cores. An alternative approach, the nitrate ^{17}O anomaly ($\Delta^{17}O$-NO_3^-, see details in Section 2.3) in atmospheric deposition, has recently been developed as a natural tracer to quantify the ecosystem-scale GNR. It is similar in some respects to the ^{15}N pool dilution method.[11−16] The $\Delta^{17}O$-NO_3^- method has been successfully used to estimate the GNR for a lake ecosystem in Japan and six urban catchments in the southwestern USA.[11,12,14] Nevertheless, the applications of the $\Delta^{17}O$-NO_3^- method are still limited, with only our previous study from the forests. Our previous study reported that the GNR ranged from 43 to 118 kg N kg^{-1} yr^{-1} for six catchments in tropical (south China) and temperate (central Japan) forests.[13] Therefore, it is desired to promote more applications of the

$\Delta^{17}O\text{-}NO_3^-$ method to estimate the ecosystem-scale GNR, especially for forest ecosystems.

Long-term atmospheric N inputs can change the ecosystem N status from N-limited to N-saturated when the availability of NH_4^+ and NO_3^- is in excess of the total combined plant and microbial N demand in the forest.[17] When N saturation of the forest ecosystems was reached, plant growth would not increase and NO_3^- leaching sharply increase.[17] This NO_3^- leaching could be significantly correlated with both bulk and throughfall N deposition fluxes.[6,18−20] Nitrification may also be promoted by long-term atmospheric N deposition because NH_4^+ in atmospheric deposition can be the substrate for nitrification. Temperate and tropical forests in the USA had high gross nitrification rates, as assessed by the ^{15}N pool dilution method.[9] Nevertheless, how GNR responds to long-term increased N deposition is poorly understood because of the scarcity of ecosystem-scale GNR measurements. As a microbially mediated process, nitrification should also be influenced by factors such as soil physicochemical properties and microbial communities.[21−23] These factors can mostly be influenced by environmental factors such as precipitation and air temperature.[21−23] Therefore, it is vital to investigate the temporal pattern of GNR and its dependence on precipitation and air temperature.

In the present study, we have determined the concentrations and $\Delta^{17}O$ of NO_3^- in precipitation and stream water over 4 years from 2014 to 2017 at a temperate forested catchment in northeastern China. The aims of this study are to clarify the forest N status and quantify the catchment-scale GNR and further to gain further insights into the internal N cycle for the study forest. The inorganic N deposition in precipitation was about 20 kg N ha^{-1} yr^{-1} to this study site.[24] We hypothesized that (1) significant stream N leaching would be observed in the study forest; (2) soil nitrification was the major contributor to stream NO_3^- export; and (3) GNR would exhibit a seasonal pattern with higher values in summer than in other seasons due to its higher temperature and precipitation amount in summer, as high temperature and precipitation favor soil microbial activities.

2. MATERIALS AND METHODS

2.1. Study Area and Sample Collection. The study area is a 536 ha forested catchment, part of the Qingyuan Forest Chinese Ecosystem Research Network (CERN), Chinese Academy of Sciences (41° 51′ N, 124° 54′ E), in the headwater region of Hun River in Liaoning Province, northeast China (Figure S1). The study area has a temperate continental monsoon climate with warm and rainy summers and cold and dry winters.[25] The frost-free period lasts 130 days on average, and the stream has an ice-bound season lasting from November to April of next year (Figure S1).[25] The catchment consists of secondary broad-leaved forests on the mountain slopes covered by 40−80 cm thick brown soil. The parent rock is composed of granite and granite-gneiss.[25] Means of soil compositions are 25.6% for sand, 51.2% for silt, and 23.2% for clay.[26] The dominant tree species are *Fraxinus rhynchophylla*, *Juglans mandshurica*, and *Phellodendron amurense*.[26]

Daily air temperature and precipitation amount were monitored at a meteorological observation station near the outlet of the studied catchment (Figure S1). Precipitation samples (*n* = 181) were collected on a daily basis during the observation period from April 2014 to December 2017 using three manual rain gauges (diameter 20 cm) installed ~500 m

away from the stream outlet of the forested catchment. The precipitation samples contained a portion of dry deposition because the rain gauges were open to the air all the time. Stream discharge (mm) at the outlet of the catchment was calculated by streamflow flux (m^3 s^{-1}), which was automatically monitored during the non-ice-bound season during 2014−2017. Stream water samples were collected from three sites along the main stream ($M_1 − M_3$) and seven tributary sites draining to the main stream ($T_1 − T_7$) (Figure S1). Stream water samples were collected twice a week at a weir (M_3 site, *n* = 235) near the outlet of the forested catchment from April 2014 to December 2017 and semimonthly in 2015 at the other sites ($M_1 − M_2$, $T_1 − T_7$ sites, *n* = 122). The collected precipitation and stream water samples were immediately analyzed for pH and filtered through 0.22 μm nylon membrane filters and then stored at −18 °C for later chemical and isotopic analysis.

2.2. Chemical and Isotopic Analysis. The NO_3^- and nitrite (NO_2^-) concentrations in the precipitation and stream water samples were determined by an ion chromatograph (Dionex ICS-600; Thermo Fisher Scientific Inc.) with an analytical precision of ±5%. Nitrate oxygen isotopes were analyzed on samples with NO_3^- concentrations higher than 0.14 mg N L^{-1}. In brief, ~100 nmol NO_3^- was initially converted to NO_2^- by cadmium powder, and NO_2^- was further reduced to N_2O by sodium azide in an acetic acid buffer.[27,28] Afterward, the produced N_2O was introduced into a gold wire oven, which was held at 875 °C for thermal decomposition of N_2O to N_2 and O_2.[29] The produced O_2 was then analyzed by an isotope ratio mass spectrometer (IsoPrime100, IsoPrime Ltd., U.K.) for its triple oxygen isotopic compositions (^{16}O, ^{17}O, ^{18}O). All analytical steps were performed simultaneously for a subset of international nitrate reference (IAEA-N3, USGS34, and USGS35) for the calibration of the $\Delta^{17}O\text{-}NO_3^-$ values.[30,31] The analytical precision of the $\Delta^{17}O\text{-}NO_3^-$ values was ±0.5‰ (based on three to five replicate analyses of international standards).

2.3. Principles of the $\Delta^{17}O\text{-}NO_3^-$ Approach and Calculations. Mass-independent fractionations during the photochemical production of NO_3^- in the atmosphere can be expressed as $\Delta^{17}O = \delta^{17}O − 0.52 \times \delta^{18}O$.[31,32] The $\Delta^{17}O$ values of atmospheric NO_3^- have previously been reported to range from 17 to 35‰.[16,31,32,34] In contrast, nitrification is a mass-dependent fractionation process and the three oxygen atoms of nitrification-produced NO_3^- are derived from O_2 and H_2O, leading to $\Delta^{17}O$ values of nitrification-derived NO_3^- close to 0‰.[35−38] Furthermore, other terrestrial N cycle processes, such as denitrification and biological uptake, follow mass-dependent fractionation and leave the $\Delta^{17}O$ signals of the remaining NO_3^- unaltered.[37,39]

For a given undisturbed forested catchment, the soil NO_3^- pool has only two NO_3^- inputs, atmospheric NO_3^- deposition and nitrification-derived NO_3^-. The $\Delta^{17}O$ values of soil NO_3^- can thus be determined using a two-source mixing model based on the isotopic mass balance

$$\Delta^{17}O_S = f_A \times \Delta^{17}O_A + f_N \times \Delta^{17}O_N \qquad (1)$$

where $\Delta^{17}O_S$, $\Delta^{17}O_A$, and $\Delta^{17}O_N$ are the $\Delta^{17}O$ values of soil NO_3^-, atmospheric NO_3^-, and nitrification-derived NO_3^-, respectively. The f_A and f_N are the fractions of atmospherically and biologically derived NO_3^-, respectively, the sum of which is 1 as shown in the following eq 2

$$f_A + f_N = F_A/(F_A + F_N) + F_N/(F_A + F_N) = 1 \qquad (2)$$

where F_A and F_N represent the flux of atmospheric NO_3^- and GNR, respectively.

To quantify the GNR, $\Delta^{17}O_S$ was considered approximately equivalent to the measured $\Delta^{17}O$ of stream NO_3^- ($\Delta^{17}O_L$) that is lost from the soil.[12,13] $\Delta^{17}O_A$ was derived from our bulk deposition samples, while $\Delta^{17}O_N$ was assumed to be 0‰.[30,39] To match the sampling frequencies for the atmospheric bulk deposition and stream water, monthly mass-weighted mean $\Delta^{17}O_A$ ($\Delta^{17}O_{Aave}$) and $\Delta^{17}O_L$ ($\Delta^{17}O_{Lave}$) were calculated according to eq 3 for $\Delta^{17}O_{ave}$[40]

$$\Delta^{17}O_{ave} = \frac{\sum_i (C_i \times V_i \times \Delta^{17}O_i)}{\sum_i (C_i \times V_i)} \qquad (3)$$

where C_i, V_i, and $\Delta^{17}O_i$ are the NO_3^- concentration, the total precipitation or streamflow volume, and the $\Delta^{17}O\text{-}NO_3^-$ value of daily bulk deposition or stream water during the ith sampling, respectively. Monthly f_N was then calculated by eq 1 using $\Delta^{17}O_{Aave}$ and $\Delta^{17}O_{Lave}$, and its temporal variability was investigated during the non-ice-bound season over the 2014–2017 period.

The monthly GNR (F_N, in units of kg N ha^{-1} month^{-1}) was then obtained by combining eqs 1–3 as follows

$$F_N = F_A \times (\Delta^{17}O_{Aave} - \Delta^{17}O_{Lave})/\Delta^{17}O_{Lave} \qquad (4)$$

where monthly F_A was calculated by multiplying the precipitation amounts by NO_3^- concentrations over the study month. Annual and monthly stream NO_3^- leaching was calculated from the monitored discharge amounts of water and stream NO_3^- concentrations during the study period. The annual GNR (units of kg N ha^{-1} yr^{-1}) was further estimated as the sum of monthly GNR during the non-ice-bound season for each year.

2.4. Statistical Analysis. One-way analysis of variance (ANOVA) was used to test if the $\Delta^{17}O\text{-}NO_3^-$ values of bulk deposition or stream water varied significantly between seasons or among years. The relationships between monthly GNR and either precipitation or air temperature were evaluated by correlation or partial correlations analysis, with $P < 0.05$ considered statistically significant. Statistical analysis was conducted using the SPSS software (SPSS 16.0 for windows, SPSS Inc., Chicago, IL).

3. RESULTS

3.1. Atmospheric NO_3^- Inputs and Stream NO_3^- Leaching of the Forest Catchment. Nitrate concentrations in bulk deposition ranged from 0.01 to 8.2 mg N L^{-1} (average 1.0 ± 1.4 mg N L^{-1}, $n = 181$) over the 4 years (Figure 1c). Annual bulk NO_3^- deposition flux ranged from 6.6 to 7.4 kg N ha^{-1} yr^{-1} (average 7.0), accounting for 32–42% of the dissolved inorganic N (DIN = NH_4^+ + NO_3^-) deposition flux (17.0–21.4 kg N ha^{-1} yr^{-1}, average 19.2 kg N ha^{-1} yr^{-1}; Table 1). Stream NO_3^- concentrations at the outlet of the forest catchment (M_3 site) ranged from 0.8 to 3.8 mg N L^{-1} (average 2.1 ± 0.6 mg N L^{-1}, $n = 235$) with a declining trend from spring to summer during each of the 4 years (Figure 1c). Nitrate concentration in the other sampling locations along the stream was 2.3–3.9 mg N L^{-1}, with most locations having higher values than that of the outlet (Figure S2). Annual stream NO_3^- leaching from the catchment ranged from 4.2 to
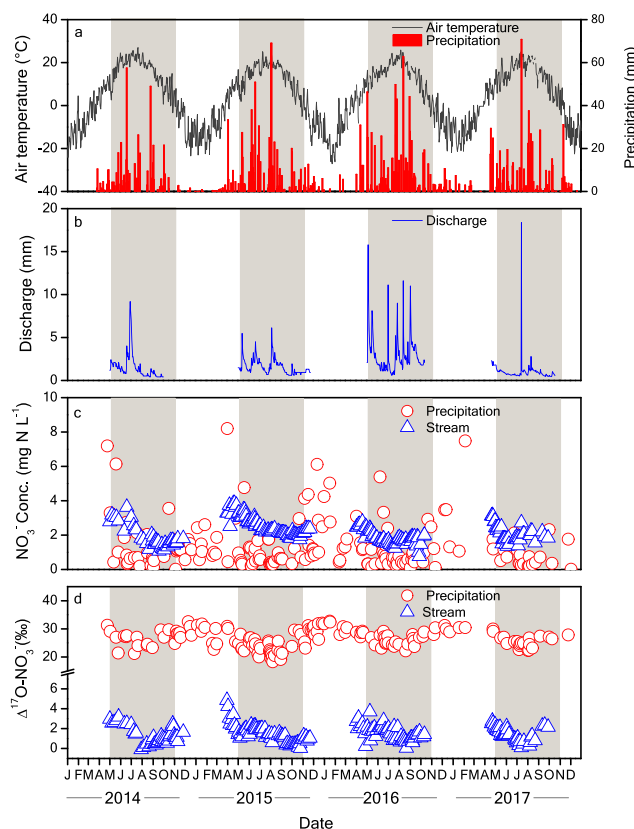

Figure 1. Daily mean air temperature and precipitation (a), daily stream discharge (b), NO_3^- concentration (c), and nitrate $\Delta^{17}O$ (d) in precipitation and stream water (M_3) from April 2014 to December 2017. The shaded areas denote the warm seasons from May to October.

8.9 kg N ha^{-1} yr^{-1}, with an average of 6.9 kg N ha^{-1} yr^{-1} over the 4 years (Table 1).

3.2. Fractional Contributions of Nitrification-Derived Nitrate to Stream Nitrate. The $\Delta^{17}O_A$ varied from 18.3 to 32.7‰ (average 26.2 ± 3.3‰, $n = 150$) and was significantly higher in cool seasons (average 29.1 ± 2.3‰) than in warm seasons (average 24.8 ± 2.6‰; Table S1 and Figure 1d). The $\Delta^{17}O_A$ was significantly correlated with daily air temperature ($n = 150$, $R^2 = 0.49$, $P < 0.001$) and NO_3^- concentration ($n = 150$, $R^2 = 0.22$, $P < 0.001$) (Figure S3). The $\Delta^{17}O_L$ ranged from −0.1 to 4.8‰ (average 1.4 ± 0.8‰, $n = 231$) with a seasonal pattern similar to that of stream NO_3^- concentrations (Figure 1d). As a result, $\Delta^{17}O_L$ was significantly correlated with stream NO_3^- concentration ($n = 231$, $R^2 = 0.25$, $P < 0.001$). $\Delta^{17}O_L$ was not correlated with stream discharge ($n = 192$, $R^2 = 0.006$, $P = 0.30$; Figure S4). During the four-year period, annual f_N ranged from 92 to 96%, while monthly f_N ranged from 89 to 99% (Table 1 and Figure 2). Monthly f_N increased during the growing season in 2014 and 2015 and increased and then decreased later during the growing season in 2016 and 2017 (Figure 2).

3.3. GNR and Its Temporal Variations Quantified by $\Delta^{17}O$. The annual GNR ranged from 71 to 120 kg N ha^{-1} yr^{-1}, with an average of 94 kg N ha^{-1} yr^{-1} over the 4 years in the forested catchment (Table 1). The ecosystem-scale GNR did not differ significantly among seasons and averaged 12, 20, and 25 kg N ha^{-1} month^{-1} in spring, summer, and autumn, respectively (Figure 3). The monthly GNR fluctuated from 1 to 60 kg N ha^{-1} month^{-1}, with no clear seasonal or interannual

Table 1. Annual Gross Nitrification Rates and Related Parameters over the Four-Year Period for the Forested Catchment[a]

year	2014	2015	2016	2017	total[b]
MAT (°C)	5.4	4.3	4.1	4.0	4.5 (0.3)
MAP (mm)	484	769	898	658	709 (87)
discharge (mm)	230	324	495	188	309 (68)
$\Delta^{17}O_A$ (‰)[c]	27.9	25.3	27.2	27.6	27.0 (0.6)
$\Delta^{17}O_L$ (‰)[c]	2.1	1.5	1.4	1.2	1.6 (0.2)
f_A (%)	7.5	5.9	5.1	4.3	5.8 (0.7)
f_N (%)	92.5	94.1	94.9	95.7	94.3 (0.7)
DIN deposition (kg N ha^{-1} yr^{-1})	20.9	21.4	17.6	17.0	19.2 (1.1)
NO_3^- deposition (kg N ha^{-1} yr^{-1})	6.6	7.4	7.2	6.9	7.0 (0.2)
NH_4^+ deposition (kg N ha^{-1} yr^{-1})	14.4	14.1	10.4	10.1	12.3 (1.1)
stream DIN leaching (kg N ha^{-1} yr^{-1})	6.6	8.3	8.9	4.2	7.0 (1.1)
stream NO_3^- leaching (kg N ha^{-1} yr^{-1})	6.5	8.1	8.9	4.2	6.9 (1.1)
stream NH_4^+ leaching (kg N ha^{-1} yr^{-1})	0.1	0.2	0.0	0.0	0.1 (0.1)
aboveground litter N (kg N ha^{-1} yr^{-1})	61.5	46.8	54.0	72.1	58.6 (5.4)
gross nitrification rate (kg N ha^{-1} yr^{-1})	71	93	90	120	94 (10)

[a]MAT, mean annual temperature; MAP, mean annual precipitation; DIN, dissolved inorganic nitrogen. [b]Mean (±1 SE, n = 4). [c]Mass-weighted.
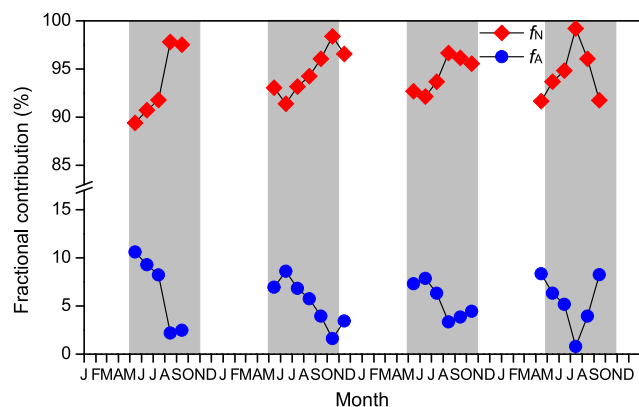

Figure 2. Monthly fractional contributions of nitrification-derived NO_3^- and bulk atmospheric NO_3^- to stream NO_3^- during the study period at the forested catchment.

Figure 3. Monthly fluxes of bulk atmospheric NO_3^- deposition (a), stream NO_3^- loss (b), and gross nitrification rate (c) at the catchment during the study period.

variations over the 4 years (Figure 3). The GNR did not correlate significantly with precipitation (n = 24, r = 0.17, P = 0.44) or with air temperature (n = 24, r = 0.06, P = 0.77; Figure 4).

4. DISCUSSION

4.1. Nitrogen Status of the Forest Ecosystem Evaluated by Stream NO_3^- Concentration and Seasonal Pattern.
According to the N saturation hypothesis (Figure S5), if judged alone from the concentration and seasonal pattern of stream NO_3^-, our study forest ecosystem may have been N-saturated (at stage 2). Stoddard (1994) proposed four N stages of the forest ecosystems according to how forests respond to chronic N additions (Figure S5b).[43] At stage 0, the N cycle is N-limited and regulated by biological uptake, and
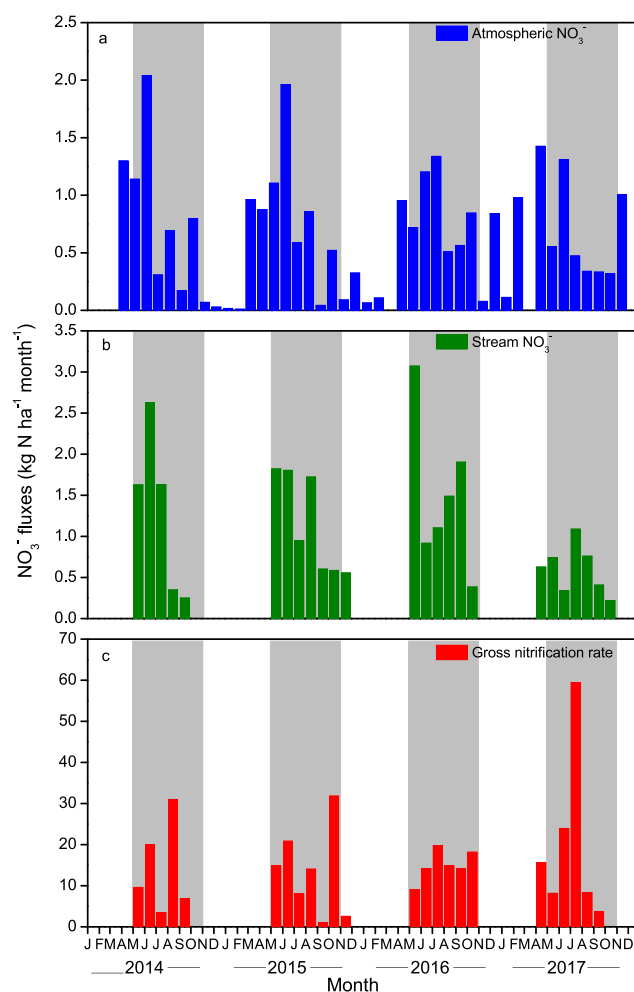
stream NO_3^- concentrations are very low throughout the growing season but slightly higher during snow melt. At stage 1, stream NO_3^- concentrations increase compared to stage 0 but are still reduced to negligible levels (near detection limit) at the peak of the growing season (maximum plant uptake period). At stage 2, the N supplies (from N deposition and mineralization) exceed the demands of plant and microbial uptake, and the N cycle is N-saturated and dominated by N loss through leaching and denitrification, with the elevated NO_3^- concentrations throughout the growing season. At stage 3, the forest ecosystem declines and becomes a net source of N rather than a sink, with extremely high stream NO_3^- concentrations year around.[42,43] At our study forest, stream NO_3^- concentrations (average 2.1 mg N L^{-1}; Figure 1c) are higher than the stream NO_3^- concentrations of 0.5−1.2 mg N L^{-1} at the Fernow Experimental Forest (diagnosed as at stage 2) in West Virginia but lower than that of 2.0−3.8 mg N L^{-1} at Dicke Bramke in Germany, which had been diagnosed as at stage 3.[43] In addition, stream NO_3^- concentrations varied seasonally over the 4 years, with slightly lower values in the growing seasons than the nongrowing seasons, which is consistent with patterns from the Fernow Experimental Forest (stage 2; Figure S5b).[43] We have estimated the total N output (via leaching and gaseous losses) to be 10.7 N ha^{-1} yr^{-1} (Table S2). This is lower than N input via precipitation, suggesting
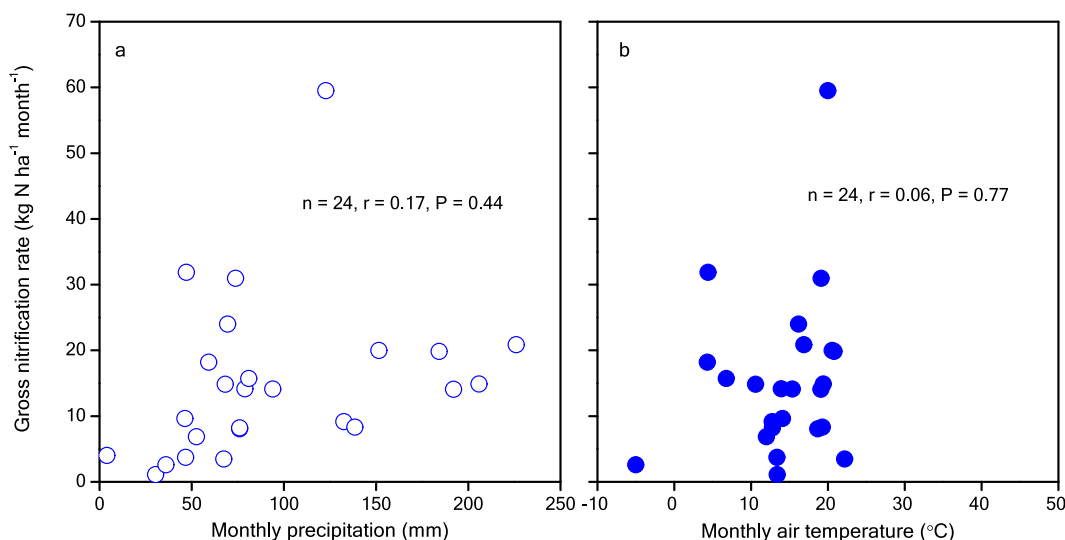
Figure 4. Relationships between monthly gross nitrification rates and monthly precipitation (a) and monthly air temperature (b). The relationships between monthly GNR and precipitation amount (or air temperature) were evaluated by the two-tailed partial correlations analyses.

that our study forest is still a N sink for atmospheric deposition, albeit with large nitrification and stream NO_3^- leaching.

4.2. Contribution of Soil Nitrification to Stream Nitrate. Since the study forest is N-saturated when evaluated with stream NO_3^- concentrations, we expected that nitrification should be an important process. At stage 2, excess N inputs, especially NH_4^+ deposition, may have increased soil nitrification. Soil NO_3^- produced from soil nitrification or from atmospheric inputs of NO_3^- can be leached to stream. The range of $\Delta^{17}O_A$ (18.3−32.7‰; Figure 1d) at our site (41 °N) is consistent with those previously reported in the mid-latitude regions, such as Lake Biwa (36 °N; 18.6 to 32.4‰) and coastal California (32 to 38 °N; 19.0 to 30.0‰).[31,41,44] In addition, $\Delta^{17}O_A$ varied seasonally, with higher values in cool seasons than in warm seasons over the four-year period, as previously reported for atmospheric NO_3^-.[31,33,34,40,41,45] The seasonal pattern is derived from the seasonal changes in the relative importance of three major pathways of nitric acid formation in the atmosphere.[33] The range of $\Delta^{17}O_L$ (−0.1−4.8‰) in our study catchment is within that reported (−1.4−6.8‰) for natural surface water.[14,39−41,46,47] The resulted annual f_N during 2014−2017 in our forested catchment (92−96%; Table 1) also coincides with those estimations of f_N in lake systems based on the $\Delta^{17}O$-NO_3^- tracer such as Lake Biwa (88−98%)[41] and close to the mean f_N of 90% for multiple mixed hardwood forest sites in the USA.[20] Monthly variations in the contributions of nitrification-derived N showed that soil nitrification contributed from 89 to 99% of stream NO_3^- (Figure 2). Therefore, our results indicate that stream NO_3^- at our forested catchment is predominantly from soil nitrification and that atmospheric NO_3^- was biologically processed before leaching to the stream.

4.3. Ecosystem-Scale GNR and Its Influencing Factors. High ecosystem-scale GNR (average 94 kg N ha^{-1} yr^{-1}) for our forested catchment further supports our hypothesis. These values are close to those in the temperate broad-leaved and coniferous forests in China and Japan (average 108 kg N ha^{-1} yr^{-1}) quantified by the same method, $\Delta^{17}O$-NO_3^-.[13] However, our quantification of the catchment-scale GNR (eqs 3 and 4) has some uncertainties. First, the sampling frequency of twice a

week on stream water may be insufficient in the rainy seasons. If the overland flow was occurring and had not been captured by sampling, the input of some atmospheric NO_3^- of high $\Delta^{17}O$ values would lead to an underestimation of the GNR.[12] The second uncertainty was from precipitation sampling. We only collected bulk precipitation. The bulk NO_3^- deposition flux should be smaller than the total NO_3^- deposition flux (wet + dry). However, most dry depositions might have been missed by our rain gauges. The ratio of dry NO_3^- deposition to wet/bulk NO_3^- deposition was reported to be 41% at rural sites in northeast China.[48] Therefore, the real GNR could be about 40% higher than that calculated with bulk NO_3^- deposition based on eq 4, suggesting that dry deposition should be considered during the quantification of the GNR using the $\Delta^{17}O$-NO_3^- method. Third, in our forested catchment, the GNR during the cool seasons was not included because there was no access to stream water samples during the ice-bound period. During the ice-bound period, the soil temperature is lower than 0 °C, which decreases microbial activity, but some NO_3^- production may be possible during this period.[49] The GNR in our forested catchment fluctuated widely and did not differ significantly between seasons (Figure 3c), which is inconsistent with the previous study.[50] The GNR values measured by the BaPS technique were significantly higher during wet seasons than during the dry seasons at two rainforest sites in Australia.[50] Insignificant seasonal pattern of the GNR in our forest site might be caused by the unmeasured GNR among the ice-bound period.

We further tested whether precipitation and air temperature significantly affected the temporal variations of GNR. Due to the significant correlation between monthly air temperature and monthly precipitation ($n = 43$, $r = 0.75$, $P < 0.001$), partial correlation analysis was conducted on monthly GNR and monthly precipitation or monthly air temperature. Precipitation can affect the GNR primarily by changing soil water-filled pore space (WFPS), and while water is necessary for microbial growth, too much water will limit nitrification.[51] In previous studies, the GNR increased with soil WFPS and then progressively declined as soils become saturated, with the optimal WFPS typically at 60−65%.[50−52] However, in this study, the monthly GNR and monthly precipitation were
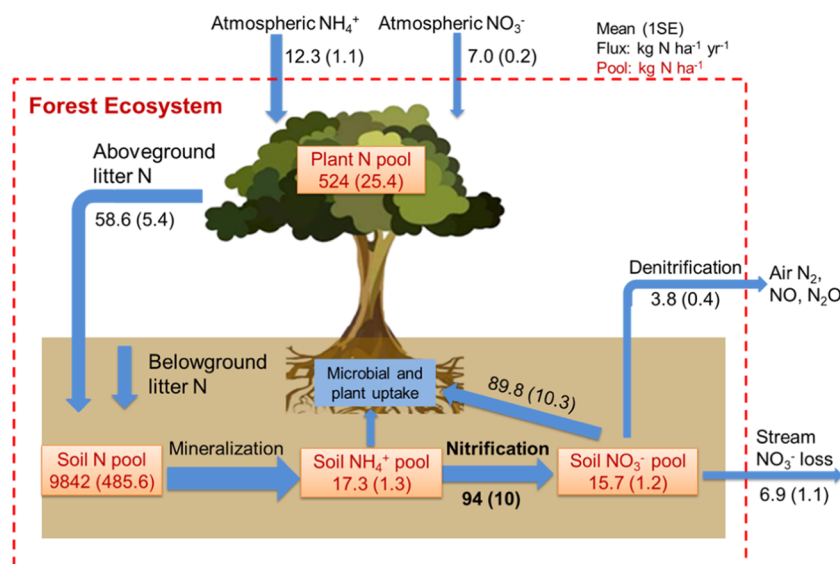
Figure 5. Simplified schematic of N cycling in the temperate forested catchment. The width of the arrows denotes the relative magnitude of the fluxes. The calculations of the fluxes of aboveground litter N, denitrification, and plant NO_3^- uptake can be found in the Supporting Information (SI).

uncorrelated ($n = 24$, $r = 0.17$, $P = 0.44$), indicating that the precipitation insignificantly affected the temporal variations of GNR in our study catchment. Meanwhile, optimal temperatures for soil nitrifier activity appears to be 15–20 °C. The GNR should increase with temperature to this optimal temperature and progressively decline afterward.[21,53−55] For example, prior studies found that the GNR increased with incubation temperature from 2 °C to 15 °C but declined with the increase in temperature from 15 to 20 °C.[21,53] Furthermore, the GNR among different temperature treatments increased in the order 15 > 40 > 5 °C.[54] However, the monthly GNR and monthly air temperature were uncorrelated ($n = 24$, $r = 0.06$, $P = 0.77$), indicating that air temperature has no straightforward impacts on temporal variations in the monthly GNR. These poor relationships are likely due to the mixing of water with different travel times, which can dilute any relationship with time-dependent parameters, namely, "the legacy effect". Stream water at the outlet is a mixture of soil water and precipitation with a continuum of travel times. Soil water may have travel times from days to months from the top of the catchment before passing the outlet.

4.4. Implications for the Internal N Cycling in the Forest Ecosystem. Nitrification is a key process of the N cycle, and GNR is crucial for the knowledge about ecosystem-scale internal N cycling under field conditions. Here, estimates of the GNR provide a more comprehensive picture for catchment-scale N cycling in the study forest (Figure 5 and Text S1). Soil NO_3^- mainly has two sources, atmospheric NO_3^- deposition and soil nitrification, and three sinks, biological (plant and microbial) uptake, denitrification, and stream leaching. After quantifying the catchment-scale GNR in the study forest ecosystem, the fluxes of denitrification and biological uptake then can be quantified by the NO_3^- isotope natural abundance approach (Figure 5 and Text S2).[13] Our results suggest that biological uptake is the most important sink of soil NO_3^-, as observed in other forests.[13] Litter N would be 117 kg N ha^{-1} yr^{-1} (Figure S6) if the N amount of underground litter was equal to that of aboveground litter,[56,57] which is comparable to soil NO_3^- consumption by plant

uptake (89.8 kg N ha^{-1} yr^{-1}; Table S2). Ecosystem N is lost by stream leaching or denitrification to the atmosphere. In the study forest, stream leaching averaged 6.9 kg N ha^{-1} yr^{-1} and denitrification was estimated to be 3.8 kg N ha^{-1} yr^{-1} (Table S2), contributing 65 and 35% of total ecosystem N loss (10.7 kg N ha^{-1} yr^{-1}), respectively (Figure 5). The total N output is 56% of the N input from bulk precipitation (19.2 kg N ha^{-1} yr^{-1}), suggesting the catchment is still a N sink for atmospheric deposition, although the forest exhibited a large stream N leaching.

■ ASSOCIATED CONTENT

Ⓢ Supporting Information

The Supporting Information is available free of charge at https://pubs.acs.org/doi/10.1021/acs.est.9b07839.

■ AUTHOR INFORMATION

Corresponding Author

Yunting Fang − *CAS Key Laboratory of Forest Ecology and Management, Institute of Applied Ecology, Chinese Academy of Sciences, Shenyang 110164, China; Key Laboratory of Stable Isotope Techniques and Applications, Shenyang, Liaoning Province 110016, China; Qingyuan Forest CERN, Chinese Academy of Sciences, Shenyang, Liaoning 110014, China;* Ⓞ orcid.org/0000-0001-7531-546X; Phone: +86-024-83970541; Email: fangyt@iae.ac.cn

Authors

Shaonan Huang − *CAS Key Laboratory of Forest Ecology and Management, Institute of Applied Ecology, Chinese Academy of Sciences, Shenyang 110164, China; Key Laboratory of Geospatial Technology for the Middle and Lower Yellow River Regions, Ministry of Education, College of Environment and Planning, Henan University, Kaifeng 475004, China*

Fan Wang − *School of Atmospheric Sciences, Guangdong Province Key Laboratory for Climate Change and Natural Disaster Studies, Sun Yat-sen University, Zhuhai, Guangdong Province 519082, China; Southern Marine Science and Engineering Guangdong Laboratory (Zhuhai), Zhuhai, Guangdong Province 519082, China*

Emily M. Elliott − *Department of Geology & Environmental Science, University of Pittsburgh, Pittsburgh, Pennsylvania 15260, United States*

Feifei Zhu − *CAS Key Laboratory of Forest Ecology and Management, Institute of Applied Ecology, Chinese Academy of Sciences, Shenyang 110164, China; Key Laboratory of Stable Isotope Techniques and Applications, Shenyang, Liaoning Province 110016, China; Qingyuan Forest CERN, Chinese Academy of Sciences, Shenyang, Liaoning 110014, China*

Weixing Zhu − *Department of Biological Sciences, Binghamton University, The State University of New York, Binghamton, New York 13902, United States*

Keisuke Koba − *Center for Ecological Research, Kyoto University, Shiga 520-2113, Japan;* ● orcid.org/0000-0003-1942-9811

Zhongjie Yu − *Department of Soil, Water, and Climate, University of Minnesota, St. Paul, Minnesota 55108, United States;* ● orcid.org/0000-0002-4935-0154

Erik A. Hobbie − *Earth Systems Research Center, University of New Hampshire, Durham, New Hampshire 03824, United States*

Greg Michalski − *Department of Chemistry, Department of Earth, Atmospheric, and Planetary Sciences, Purdue University, West Lafayette, Indiana 47907, United States*

Ronghua Kang − *CAS Key Laboratory of Forest Ecology and Management, Institute of Applied Ecology, Chinese Academy of Sciences, Shenyang 110164, China; Qingyuan Forest CERN, Chinese Academy of Sciences, Shenyang, Liaoning 110014, China*

Anzhi Wang − *CAS Key Laboratory of Forest Ecology and Management, Institute of Applied Ecology, Chinese Academy of Sciences, Shenyang 110164, China*

Jiaojun Zhu − *CAS Key Laboratory of Forest Ecology and Management, Institute of Applied Ecology, Chinese Academy of Sciences, Shenyang 110164, China; Qingyuan Forest CERN, Chinese Academy of Sciences, Shenyang, Liaoning 110014, China*

Shenglei Fu − *Key Laboratory of Geospatial Technology for the Middle and Lower Yellow River Regions, Ministry of Education, College of Environment and Planning, Henan University, Kaifeng 475004, China*

Complete contact information is available at:
https://pubs.acs.org/10.1021/acs.est.9b07839

Author Contributions

Y.F. conceived the study; S.H. collected the samples and did chemical and isotope analyses; Y.F., S.H., F.W., and E.M.E. analyzed the data and wrote the paper with inputs from all co-authors.

Notes

The authors declare no competing financial interest.

■ REFERENCES

(1) Galloway, J. N.; Townsend, A. R.; Jan Willem, E.; Mateete, B.; Zucong, C.; Freney, J. R.; Martinelli, L. A.; Seitzinger, S. P.; Sutton, M. A. Transformation of the nitrogen cycle: recent trends, questions, and potential solutions. *Science* **2008**, *320*, 889−892.

(2) Fowler, D.; Steadman, C. E.; Stevenson, D.; Coyle, M.; Rees, R. M.; Skiba, U. M.; Sutton, M. A.; Cape, J. N.; Dore, A. J.; Vieno, M. Effects of global change during the 21st century on the nitrogen cycle. *Atmos. Chem. Phys.* **2015**, *15*, 1747−1868.

(3) Vitousek, P. M.; Aber, J. D.; Howarth, R. W.; Likens, G. E.; Matson, P. A.; Schindler, D. W.; Schlesinger, W. H.; Tilman, D. G. Human alteration of the global nitrogen cycle: sources and consequences. *Ecol. Appl.* **1997**, *7*, 737−750.

(4) Matson, P.; Lohse, K. A.; Hall, S. J. The globalization of nitrogen deposition: consequences for terrestrial ecosystems. *Ambio* **2002**, *31*, 113−119.

(5) Bowman, W. D.; Cleveland, C. C.; Halada, Ĺ.; Hreško, J.; Baron, J. S. Negative impact of nitrogen deposition on soil buffering capacity. *Nat. Geosci.* **2008**, *1*, 767−770.

(6) Dise, N. B.; Rothwell, J. J.; Gauci, V.; van der Salm, C.; de Vries, W. Predicting dissolved inorganic nitrogen leaching in European forests using two independent databases. *Sci. Total Environ.* **2009**, *407*, 1798−808.

(7) Stevens, C. J.; Duprè, C.; Dorland, E.; Gaudnik, C.; Gowing, D. J. G.; Bleeker, A.; Diekmann, M.; Alard, D.; Bobbink, R.; Fowler, D. The impact of nitrogen deposition on acid grasslands in the Atlantic region of Europe. *Environ. Pollut.* **2011**, *159*, 2243−2250.

(8) Davidson, E. A.; Hart, S. C.; Shanks, C. A.; Firestone, M. K. Measuring gross nitrogen mineralization, immobilization, and nitrification by 15N isotopic pool dilution in intact soil cores. *J. Soil Sci.* **1991**, *42*, 335−349.

(9) Stark, J. M.; Hart, S. C. High rates of nitrification and nitrate turnover in undisturbed coniferous forests. *Nature* **1997**, *385*, 61−64.

(10) Ingwersen, J.; Butterbach-Bahl, K.; Gasche, R.; Papen, H.; Richter, O. Barometric process separation: new method for quantifying nitrification, denitrification, and nitrous oxide sources in soils. *Soil Sci. Soc. Am. J.* **1999**, *63*, 117−128.

(11) Tsunogai, U.; Daita, S.; Komatsu, D.; Nakagawa, F.; Tanaka, A. Quantifying nitrate dynamics in an oligotrophic lake using $\Delta^{17}O$. *Biogeosciences* **2011**, *8*, 687−702.

(12) Riha, K. M.; Michalski, G.; Gallo, E. L.; Lohse, K. A.; Brooks, P. D.; Meixner, T. High atmospheric nitrate inputs and nitrogen turnover in semi-arid urban catchments. *Ecosystems* **2014**, *17*, 1309−1325.

(13) Fang, Y.; Koba, K.; Makabe, A.; Takahashi, C.; Zhu, W.; Hayashi, T.; Hokari, A. A.; Urakawa, R.; Bai, E.; Houlton, B. Z.; Xi, D.; Zhang, S.; Matsushita, K.; Tu, Y.; Liu, D.; Zhu, F.; Wang, Z.;

Zhou, G.; Chen, D.; Makita, T.; Toda, H.; Liu, X.; Chen, Q.; Zhang, D.; Li, Y.; Yoh, M. Microbial denitrification dominates nitrate losses from forest ecosystems. *Proc. Natl. Acad. Sci. U.S.A.* **2015**, *112*, 1470−4.

(14) Tsunogai, U.; Miyauchi, T.; Ohyama, T.; Komatsu, D. D.; Ito, M.; Nakagawa, F. Quantifying nitrate dynamics in a mesotrophic lake using triple oxygen isotopes as tracers. *Limnol. Oceanogr.* **2018**, *63*, S458−S476.

(15) Yu, Z.; Elliott, E. M. Probing soil nitrification and nitrate consumption using $\Delta17O$ of soil nitrate. *Soil Biol. Biochem.* **2018**, *127*, 187−199.

(16) Bourgeois, I.; Savarino, J.; Caillon, N.; Angot, H.; Barbero, A.; Delbart, F.; Voisin, D.; Clément, J.-C. Tracing the fate of atmospheric nitrate in a subalpine watershed using $\Delta^{17}O$. *Environ. Sci. Technol.* **2018**, *52*, 5561−5570.

(17) Aber, J. D.; Nadelhoffer, K. J.; Steudler, P.; Melillo, J. M. Nitrogen saturation in northern forest ecosystems. *BioScience* **1989**, *39*, 378−286.

(18) Gundersen, P. Nitrogen deposition and leaching in European forests—preliminary results from a data compilation. *Water Air Soil Pollut.* **1995**, *85*, 1179−1184.

(19) Burns, D. A.; Kendall, C. Analysis of $\delta15N$ and $\delta18O$ to differentiate NO3− sources in runoff at two watersheds in the Catskill Mountains of New York. *Water Resour. Res.* **2002**, *38*, 9-1−9-11.

(20) Rose, L. A.; Sebestyen, S. D.; Elliott, E. M.; Koba, K. Drivers of atmospheric nitrate processing and export in forested catchments. *Water Resour. Res.* **2015**, *51*, 1333−1352.

(21) Compton, J. E.; Boone, R. D. Soil nitrogen transformations and the role of light fraction organic matter in forest soils. *Soil Biol. Biochem.* **2002**, *34*, 933−943.

(22) Templer, P.; Findlay, S.; Lovett, G. Soil microbial biomass and nitrogen transformations among five tree species of the Catskill Mountains, New York, USA. *Soil Biol. Biochem.* **2003**, *35*, 607−613.

(23) Grenon, F.; Bradley, R.; Titus, B. Temperature sensitivity of mineral N transformation rates, and heterotrophic nitrification: possible factors controlling the post-disturbance mineral N flush in forest floors. *Soil Biol. Biochem.* **2004**, *36*, 1465−1474.

(24) Huang, S.; Elliott, E. M.; Felix, J. D.; Pan, Y.; Liu, D.; Li, S.; Li, Z.; Zhu, F.; Zhang, N.; Fu, P. Seasonal pattern of ammonium 15N natural abundance in precipitation at a rural forested site and implications for NH3 source partitioning. *Environ. Pollut.* **2019**, *247*, 541−549.

(25) Zhu, J.; Mao, Z.; Hu, L.; Zhang, J. Plant diversity of secondary forests in response to anthropogenic disturbance levels in montane regions of northeastern China. *J. For. Res.* **2007**, *12*, 403−416.

(26) Yang, K.; Zhu, J.; Zhang, M.; Yan, Q.; Sun, O. J. Soil microbial biomass carbon and nitrogen in forest ecosystems of Northeast China: a comparison between natural secondary forest and larch plantation. *J. Plant Ecol.* **2010**, *3*, 175−182.

(27) McIlvin, M. R.; Altabet, M. A. Chemical conversion of nitrate and nitrite to nitrous oxide for nitrogen and oxygen isotopic analysis in freshwater and seawater. *Anal. Chem.* **2005**, *77*, 5589−5595.

(28) Tu, Y.; Fang, Y.; Liu, D.; Pan, Y. Modifications to the azide method for nitrate isotope analysis. *Rapid Commun. Mass Spectrom.* **2016**, *30*, 1213−1222.

(29) Smirnoff, A.; Savard, M. M.; Vet, R.; Simard, M. C. Nitrogen and triple oxygen isotopes in near-road air samples using chemical conversion and thermal decomposition. *Rapid Commun. Mass Spectrom.* **2012**, *26*, 2791−2804.

(30) Miller, M. F. Isotopic fractionation and the quantification of 17O anomalies in the oxygen three-isotope system: an appraisal and geochemical significance. *Geochim. Cosmochim. Acta* **2002**, *66*, 1881−1889.

(31) Michalski, G.; Scott, Z.; Kabiling, M.; Thiemens, M. H. First measurements and modeling of $\Delta17O$ in atmospheric nitrate. *Geophys. Res. Lett.* **2003**, *30*, No. 175.

(32) Thiemens, M. H. Mass-independent isotope effects in planetary atmospheres and the early solar system. *Science* **1999**, *283*, 341−345.

(33) Alexander, B.; Hastings, M.; Allman, D.; Dachs, J.; Thornton, J.; Kunasek, S. Quantifying atmospheric nitrate formation pathways based on a global model of the oxygen isotopic composition (Δ 17 O) of atmospheric nitrate. *Atmos. Chem. Phys.* **2009**, *9*, 5043−5056.

(34) Savard, M. M.; Cole, A. S.; Vet, R.; Smirnoff, A. The Δ 17 O and δ 18 O values of atmospheric nitrates simultaneously collected downwind of anthropogenic sources−implications for polluted air masses. *Atmos. Chem. Phys.* **2018**, *18*, 10373−10389.

(35) Aleem, M.; Hoch, G.; Varner, J. Water as the source of oxidant and reductant in bacterial chemosynthesis. *Proc. Natl. Acad. Sci. U.S.A.* **1965**, *54*, 869.

(36) Andersson, K. K.; Hooper, A. B. O2 and H2O are each the source of one O in NO−2 produced from NH3 by Nitrosomonas: 15N-NMR evidence. *FEBS Lett.* **1983**, *164*, 236−240.

(37) Young, E. D.; Yeung, L. Y.; Kohl, I. E. On the $\Delta17O$ budget of atmospheric O2. *Geochim. Cosmochim. Acta* **2014**, *135*, 102−125.

(38) Thiemens, M. H. History and applications of mass-independent isotope effects. *Annu. Rev. Earth Planet. Sci.* **2006**, *34*, 217−262.

(39) Michalski, G.; Meixner, T.; Fenn, M.; Hernandez, L.; Sirulnik, A.; Allen, E.; Thiemens, M. Tracing atmospheric nitrate deposition in a complex semiarid ecosystem using $\Delta17O$. *Environ. Sci. Technol.* **2004**, *40*, 2175−2181.

(40) Tsunogai, U.; Komatsu, D. D.; Daita, S.; Kazemi, G.; Nakagawa, F.; Noguchi, I.; Zhang, J. Tracing the fate of atmospheric nitrate deposited onto a forest ecosystem in Eastern Asia using Δ 17 O. *Atmos. Chem. Phys.* **2010**, *10*, 1809−1820.

(41) Tsunogai, U.; Miyauchi, T.; Ohyama, T.; Komatsu, D. D.; Nakagawa, F.; Obata, Y.; Sato, K.; Ohizumi, T. Accurate and precise quantification of atmospheric nitrate in streams draining land of various uses by using triple oxygen isotopes as tracers. *Biogeosciences* **2016**, *13*, 3441−3459.

(42) Aber, J. D. Nitrogen cycling and nitrogen saturation in temperate forest ecosystems. *Trends Ecol. Evol.* **1992**, *7*, 220−224.

(43) Stoddard, J. L. Long-term changes in watershed retention of nitrogen: its causes and aquatic consequences. *ACS Adv. Chem. Series* **1994**, *237*, 223−284.

(44) Vicars, W.; Morin, S.; Savarino, J.; Wagner, N.; Erbland, J.; Vince, E.; Martins, J.; Lerner, B.; Quinn, P.; Coffman, D. Spatial and diurnal variability in reactive nitrogen oxide chemistry as reflected in the isotopic composition of atmospheric nitrate: Results from the CalNex 2010 field study. *J. Geophys. Res.: Atmos.* **2013**, *118*, 10567−10588.

(45) Ishino, S.; Hattori, S.; Savarino, J.; Jourdain, B.; Preunkert, S.; Legrand, M.; Caillon, N.; Barbero, A.; Kuribayashi, K.; Yoshida, N. Seasonal variations of triple oxygen isotopic compositions of atmospheric sulfate, nitrate, and ozone at Dumont d'Urville, coastal Antarctica. *Atmos. Chem. Phys.* **2017**, *17*, 3713−3727.

(46) Liu, T.; Wang, F.; Michalski, G.; Xia, X.; Liu, S. Using 15N, 17O, and 18O to determine nitrate sources in the Yellow River, China. *Environ. Sci. Technol.* **2013**, *47*, 13412−13421.

(47) Rose, L. A.; Elliott, E. M.; Adams, M. B. Triple nitrate isotopes indicate differing nitrate source contributions to streams across a nitrogen saturation gradient. *Ecosystems* **2015**, *18*, 1209−1223.

(48) Xu, W.; Luo, X.; Pan, Y.; Zhang, L.; Tang, A.; Shen, J.; Zhang, Y.; Li, K.; Wu, Q.; Yang, D. Quantifying atmospheric nitrogen deposition through a nationwide monitoring network across China. *Atmos. Chem. Phys.* **2015**, *15*, 12345−12360.

(49) Isobe, K.; Ikutani, J.; Fang, Y.; Yoh, M.; Mo, J.; Suwa, Y.; Yoshida, M.; Senoo, K.; Otsuka, S.; Koba, K. Highly abundant acidophilic ammonia-oxidizing archaea causes high rates of nitrification and nitrate leaching in nitrogen-saturated forest soils. *Soil Biol. Biochem.* **2018**, *122*, 220−227.

(50) Kiese, R.; Hewett, B.; Butterbach-Bahl, K. Seasonal dynamic of gross nitrification and N 2 O emission at two tropical rainforest sites in Queensland, Australia. *Plant Soil* **2008**, *309*, 105−117.

(51) Neill, C.; Piccolo, M. C.; Melillo, J. M.; Steudler, P. A.; Cerri, C. C. Nitrogen dynamics in Amazon forest and pasture soils measured by 15N pool dilution. *Soil Biol. Biochem.* **1999**, *31*, 567−572.

(52) Breuer, L.; Kiese, R.; Butterbach-Bahl, K. Temperature and moisture effects on nitrification rates in tropical rain-forest soils. *Soil Sci. Soc. Am. J.* **2002**, *66*, 834−844.

(53) Stottlemyer, R.; Toczydlowski, D. Nitrogen mineralization in a mature boreal forest, Isle Royale, Michigan. *J. Environ. Qual.* **1999**, *28*, 709−720.

(54) Zaman, M.; Chang, S. Substrate type, temperature, and moisture content affect gross and net N mineralization and nitrification rates in agroforestry systems. *Biol. Fertil. Soils* **2004**, *39*, 269−279.

(55) Kuroiwa, M.; Koba, K.; Isobe, K.; Tateno, R.; Nakanishi, A.; Inagaki, Y.; Toda, H.; Otsuka, S.; Senoo, K.; Suwa, Y. Gross nitrification rates in four Japanese forest soils: heterotrophic versus autotrophic and the regulation factors for the nitrification. *J. For. Res.* **2011**, *16*, 363−373.

(56) Bowden, R. D.; Nadelhoffer, K. J.; Boone, R. D.; Melillo, J. M.; Garrison, J. B. Contributions of aboveground litter, belowground litter, and root respiration to total soil respiration in a temperate mixed hardwood forest. *Can. J. For. Res.* **1993**, *23*, 1402−1407.

(57) Sulzman, E. W.; Brant, J. B.; Bowden, R. D.; Lajtha, K. Contribution of aboveground litter, belowground litter, and rhizosphere respiration to total soil CO_2 efflux in an old growth coniferous forest. *Biogeochemistry* **2005**, *73*, 231−256.